Applied Catalysis B: Environmental 119–120 (2012) 207–216

Contents lists available at SciVerse ScienceDirect

Applied Catalysis B: Environmental

journal homepage: www.elsevier.com/locate/apcatb

On the reducibility of sulfated Pt/$Ce_XZr_{1-X}O_2$ solids: A coupled thermogravimetric FT-IR study using CO as the reducing agent

P. Bazin[a,*], O. Saur[a], O. Marie[a], M. Daturi[a], J.C. Lavalley[a], A.M. Le Govic[b], V. Harlé[b], G. Blanchard[b,1]

[a] Laboratoire Catalyse et Spectrochimie, ENSICAEN, Université de Caen, CNRS, 6 Bd Maréchal Juin, F-14050 Caen, France
[b] Rhodia Recherches, 52 rue de La Haie-Coq, 93308 Aubervilliers, France

ARTICLE INFO

Article history:
Received 18 October 2011
Received in revised form 22 February 2012
Accepted 28 February 2012
Available online 7 March 2012

Keywords:
Three way catalysts
Oxygen storage capacity
Ceria–zirconia
Platinum
Sulfate
Sulfur dioxide
Carbon monoxide
IR spectroscopy
Thermogravimetry

ABSTRACT

The reducibility of sulfate species by CO was studied over ceria and $Ce_{0.63}Zr_{0.37}O_2$ mixed oxide with or without platinum, using infrared spectroscopy and thermogravimetry. The mechanism for sulfate reduction appeared to be based on three main points. Firstly, the exchange between surface and bulk-like sulfate species is required. The sulfate reduction indeed occurs at the oxide surface and bulk-like species need to migrate toward the surface to be further reduced. Secondly, it was observed that surface sulfate species are more easily reduced by CO on the reduced oxide. Therefore, platinum loading which favors the oxide reduction, also favors the sulfate reduction by CO. Finally, the reduction of sulfated Pt-free samples occurs in only one step, which is linked to the own reducibility of the surface sulfate species, probably through a direct interaction with CO. The amount of sulfur stored from sulfate reduction with CO is markedly more important than the one detected from reduction with H_2. Furthermore, the oxygen storage capacity (OSC) for sulfated samples is higher than the one for sulfate-free samples. This is tentatively explained by the partial replacement of oxygen by sulfur atoms in the compound lattice.

1. Introduction

Ceria–zirconia mixed oxides are currently important components of new type three way catalysts (TWCs) mainly due to their oxygen storage capacity (OSC) [1,2]. The addition of zirconia to ceria indeed improves both the thermal stability at high temperatures [3,4] and the associated OSC [5–7]. Platinum is also a standard component in TWCs formulation as a consequence of its efficiency both in CO and hydrocarbons oxidation [8] and NO conversion [9]. A major problem for the three way catalysts lies in the presence of sulfur oxide arising from lubricants and fuel combustion, which leads to sulfate formation and finally decreases the overall catalyst performance. Results have shown that the presence of Pt enhances the SO_x storage capacity [10,14]. In previous works [11–14], the interaction of H_2 with sulfated ceria–zirconia mixed oxides using infrared spectroscopy and thermogravimetric measurements was reported. Only surface sulfate species were observed over pure zirconia whatever the surface area, while bulk-like sulfates were also formed on ceria and CeO_2–ZrO_2 mixed oxide. For any studied catalyst, platinum was shown to favor the reducibility of both sulfate species when H_2 was used as the reducing agent. It was furthermore evidenced that the sulfate reduction occurs at the oxide surface, and that the vacant surface sites are subsequently repopulated upon bulk-like species migration. The bulk-like sulfate species thus act as a reservoir which feeds the superficial reduction sites. When platinum is present, the sulfate reduction by H_2 occurs in two steps. The first one, which occurs in the low temperature range (423–523 K), corresponds to the partial reduction of both oxide and surface sulfate species. It is worth noting that the temperature typical for this first step decreases with higher Zr-content (within 50% of Zr in the solid solution). This must be related to the increase of oxygen mobility upon Zr introduction as 'defect' sites in the ceria structure. The second step, which takes place at higher temperatures (623–723 K), corresponds to the complete reduction of both sulfate species (surface and bulk-like ones). In this latter case, zirconium addition increases the temperature of the second step on-set: the sulfate migration seems to be hindered. Moreover, the sulfate reduction by hydrogen was reported to yield H_2S and sulfur species which keep adsorbed on platinum and oxide surface probably in the form of cerium oxysulfur [13]. It was also determined that the amount of stored sulfur is closely linked to the sample specific surface area. Finally, even if the oxide reduction is always concomitant to that of sulfates, thermogravimetric analysis was shown to represent a reliable tool for the evaluation of sulfated ceria–zirconia mixed oxides OSC.

* Corresponding author. Fax: +33 2 31 45 28 22.
E-mail address: philippe.bazin@ensicaen.fr (P. Bazin).
[1] Current address: Sciences et Technologies Emergentes pour le Post traitement, PSA, Centre Technique de Velizy, Route de Gisy, 78943 Vélizy Villacoublay, France

0926-3373/$ – see front matter © 2012 Elsevier B.V. All rights reserved.
doi:10.1016/j.apcatb.2012.02.037

Additionally to H_2, carbon monoxide, arising from incomplete combustion, also represents a reducing agent available in the exhaust flow. In a recent study dealing with the reducibility of aged $CeZrO_2$ mixed oxide samples, Yeste et al. indeed observed, in the low-temperature range ($T \leq 773$ K), that the OSC values are significantly larger when using CO rather than H_2 as a reducer [15]. Moreover, Luo et al. have observed that all of the sulfates on Pd/Ceria samples are reduced to Ce_2O_2S with CO and to a Ce_2O_2S/H_2S mixture when H_2 was used as reducing agent [16]. CO and H_2 may therefore interact distinctly with sulfate species supported on ceria–zirconia mixed samples. The goal of the present paper is thus to compare the CO assisted reduction of sulfate species formed from SO_2 oxidation over ceria and ceria–zirconia mixed oxides, with and without platinum, in order to evaluate both the influence of Zr addition on sulfur storage, the role of the metallic phase and the differences between CO and H_2 as reducing agents.

2. Experimental

2.1. Materials

Ceria (CeO_2) and ceria–zirconia mixed oxide ($CeZrO_2$) were obtained by a Rhodia proprietary process, using a precipitation route from nitrate precursors [14]. The composition of the mixed oxide is 63 at% cerium and 37 at% zirconium and the Pt loading (when relevant) is 0.5 wt%. These data together with the specific areas of the oxides measured by the BET method are reported in Table 1. The suffix —S was then added for labeling the sulfated samples.

2.2. Infrared study

Powders were pressed into 16 mm diameter self-supported wafers in order to work in the transmission mode. Wafers, made from approximately 20 mg of powder, were further treated in situ in a quartz cell equipped with KBr windows. A calibrated small volume ($\sim$1.5 cm^3) and a pressure gauge allowed the accurate quantification of the amount of species introduced in the cell. Spectra were recorded with a Nicolet Magna 550 FTIR spectrometer (DTGS detector, resolution 4 cm^{-1}, 64 scans/spectrum) after quenching the sample at room temperature (RT). In order to decrease the amount of water and carbon dioxide in the infrared beam, the spectrometer and sample compartment were purged with H_2O and CO_2 free air. The spectra were further processed using the OMNIC® software.

All the samples were first submitted to a standard cleaning pre-treatment for the removal of any remaining impurities. This pre-treatment consists in a heating at 723 K under oxygen for 2 h followed by an evacuation ($\sim 10^{-4}$ Pa) at the same temperature.

The sulfating was performed at 673 K by introducing 600 μmol g^{-1} of SO_2 into the cell in the presence of a large O_2 excess (equilibrium pressure ≈6.5 kPa) followed by an evacuation at the same temperature.

For the study of sulfates reduction, a large excess of CO (equilibrium pressure ≈2.7 kPa) was introduced at RT into the cell. The wafer was then heated for 30 min under this environment at increasing temperatures (323, 423, 523, 623, 723 and 773 K) and further evacuated for 15 min at each of these temperatures. Carbon monoxide is not only an efficient reducing agent but also a probe molecule which provides distinct information on the support acidity and on the metallic phase oxidation state and morphology depending on the interaction conditions. Three spectra were thus recorded for each reduction temperature (noted T_{red}) in order to obtain the maximum of information about the samples properties. The first one was recorded at RT after the reducing treatment under CO ($P \approx 2.7$ kPa – 30 min) but before any evacuation. The second spectrum was recorded after evacuation at RT and the third after evacuation at T_{red}.

2.3. Thermogravimetric study

For gravimetric measurements, a Mc Bain thermobalance (for which the weight variation is evaluated by the stretching of a quartz spring) was used. The powders were pressed (ca. 400 mg), activated and sulfated in conditions similar to those applied for the IR study. The origin (zero) of the weight variation scale corresponds to the weight recorded after the standard cleaning pre-treatment described above. For the reduction study, a large excess of CO (equilibrium pressure ~ 2.7 kPa) was introduced in the thermobalance at RT; the sample was then heated to 773 K (0.5 K min^{-1}) and kept at 773 K until a constant weight was reached.

2.4. Temperature programmed reduction by CO

The temperature programmed reductions by CO (TPR_{CO}) were performed in a conventional system (quartz tubular reactor) allowing the continuous analysis of the effluents via a quadripolar mass spectrometer (MS). Sulfate free samples (500 mg) were first pretreated in situ at 773 K under N_2 (25 ml min^{-1}) and O_2 (5 ml min^{-1}) for 2 h, the gas was then switched to pure N_2 for 0.5 h before the sample was cooled to 323 K. The TPR_{CO} started upon switching to N_2 (25 ml min^{-1}) and CO (5 ml min^{-1}) at 323 K while heating up to 773 K (2.5 K min^{-1}). The sample was held at this temperature for 1 h. In the case of sulfated samples, the sulfating was preliminary performed by heating 600 μmol g^{-1} of SO_2 in the presence of a large O_2 excess ($P \sim 6.5$ kPa) at 673 K. The sulfated samples were then purged under pure N_2 at 673 K before cooling down to 323 K and finally starting the TPR_{CO} described above.

3. Results and discussion

Similar experiments were undertaken for CeO_2 and $CeZrO_2$, sulfated or not (results concerning sulfate-free samples are depicted in Supporting information), with or without Pt, aiming at discerning precisely the differences between the support reduction and the sulfate reduction by CO and the role played by both the platinum and the sample composition.

3.1. CO reduction of sulfated CeO_2

Fig. 1A shows the spectra of CeO_2-S after treatment under CO upon increasing temperatures in complementary spectral ranges. The spectrum of CeO_2 sulfated by SO_2 at 673 K and then evacuated at the same temperature (Fig. 1A-IIa) displays bands at 1400, 1372, 1170, 1058 and 986 cm^{-1}. The two first peaks at 1400 and 1372 cm^{-1} [ν(S=O)] and the two last peaks at 1058 and 986 cm^{-1} [ν(S=O)] are due to surface sulfate species, while the third at 1170 cm^{-1} corresponds to a bulk-like one [11–14]. The evolution of the spectra upon increasing T_{red} is detailed below for each informative region:

3.1.1. Carbonate–sulfate region (Fig. 1A-II: 1700–800 cm^{-1} range)

The appearance of sharp peaks at 1578 and 1368 cm^{-1}, between 423 and 523 K, indicates the formation of formate species arising from CO interaction with hydroxyl groups [17–22], as confirmed by the simultaneous rise of bands at 2946 and 2853 cm^{-1} (not shown). The set of bands at 1452, 1375, 1072 [$\nu(CO_3)$] and 856 cm^{-1} [$\pi(CO_3)$] that are clearly present after CeO_2-S reduction and evacuation at 723 and 773 K are assigned to polydentate carbonate

Table 1
Main characteristics of the investigated samples.

Samples	Atomic ratio		Weight ratio		Pt loading (wt%)	Specific area ($m^2\ g^{-1}$)
	Ce (at%)	Zr (at%)	CeO_2 (wt%)	ZrO_2 (wt%)		
CeO_2	100	0	100	0	0	170
$CeZrO_2$	63	37	70	30	0	137
Pt/CeO_2	100	0	100	0	0.5	147
$Pt/CeZrO_2$	63	37	70	30	0.5	107

species [20]. Monodentate carbonate species could be an alternative assignment to these bands regarding their wavenumbers, however monodentate species are unstable at such high temperatures [18,20]. These polydentate species may already have formed at T_{red} = 423 K (spectrum Fig. 1A-IIc), taking into account the presence of the band at 1462 cm^{-1} on the corresponding spectrum. Surface sulfate species (bands at 1400 and 1372 cm^{-1}) and bulk-like species (band at 1170 cm^{-1}) do not seem to be affected by CO at temperatures below 623 K. Nevertheless, the increase of bands due to carbonates and formates in the 1600–1300 cm^{-1} range may mask some surface sulfate alteration at T_{red} < 623 K. When T_{red} reaches 673 K (spectrum Fig. 1A-IIf), a strong decrease of the intensity of bands due to both surface and bulk-like sulfate species takes place. Finally, at T_{red} = 723 K, no significant bands associated to sulfates remain. It can thus be concluded that CO is able to reduce any sulfate species at 723 K.

3.1.2. *Adsorbed CO region (Fig. 1A-I: 2400–1900 cm^{-1} range)*

The band at 2191 cm^{-1} detected after CO treatment at 323 K (and which vanishes upon RT evacuation) is assigned to CO interacting with ceria cationic sites (Ce^{4+}). For the non-sulfated CeO_2 (see Supporting information, Fig. S1A-Ia), the corresponding adsorbed CO stretching vibration is detected at 2172 cm^{-1}. In a previous study, Badri [22] observed a similar shift toward higher wavenumbers (+17 cm^{-1}) after CO was adsorbed on chlorinated ceria when compared to pure ceria. This effect is due to the electron acceptor

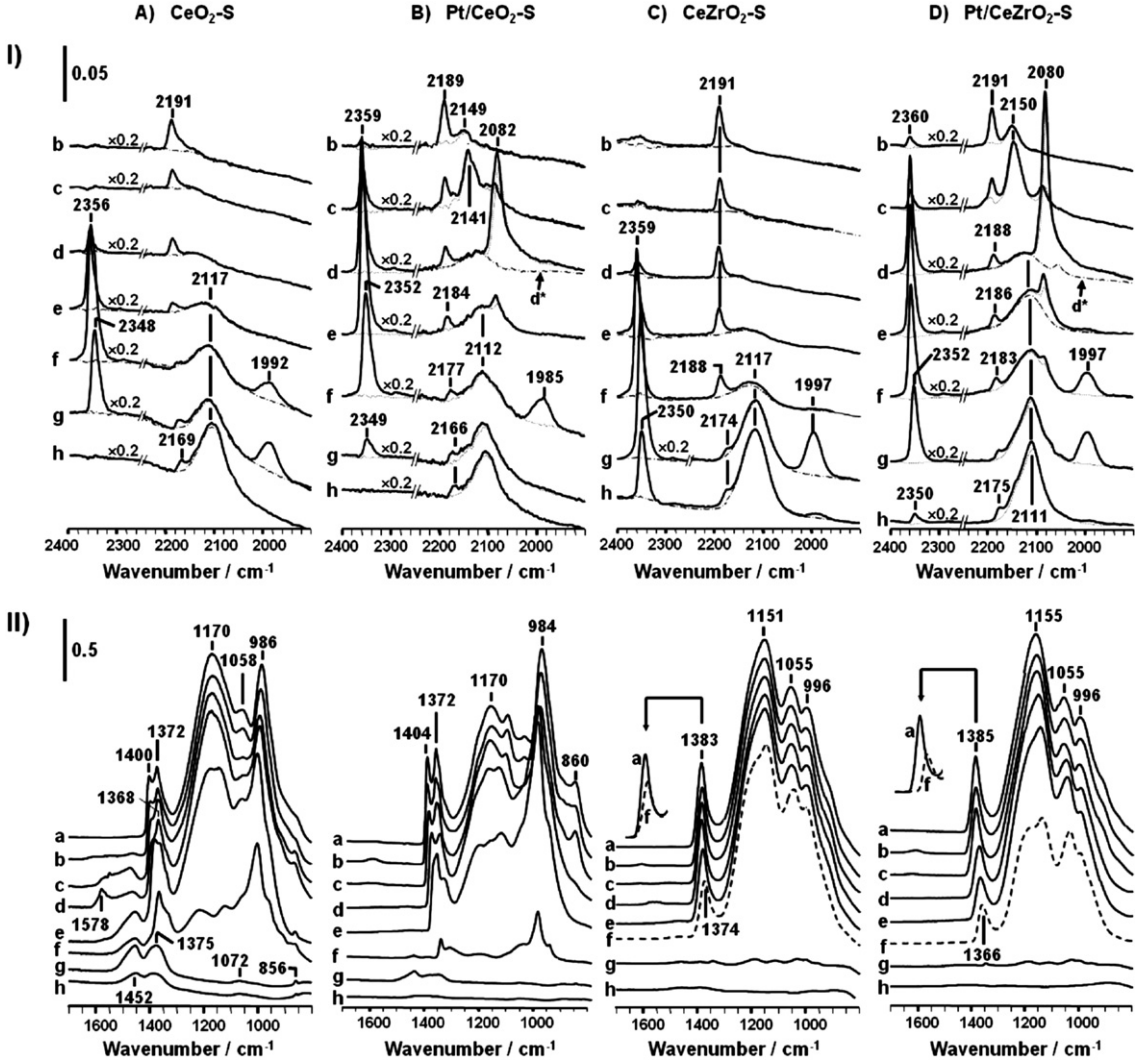

Fig. 1. IR spectra of sulfated samples recorded after (a) sulfating at 673 K by SO_2 (600 μmol g^{-1}) and O_2, then heated under CO (30 min) at T_{red} equal to (b) 323, (c) 423, (d) 523, (e) 623, (f) 673, (g) 723 and (h) 773 K. Part I: solid lines correspond to spectra recorded at room temperature after CO treatment without evacuation and dotted lines correspond to spectra recorded after evacuation at room temperature. Parts II and Id*: spectra were recorded after evacuation at T_{red}.

properties of chlorine, which impose to the cerium cations to further attract the CO electron pair. Similarly, when CO interacts with CeO_2-S, the presence of sulfate species leads to an upwards shift of around +19 cm^{-1} [23]. Therefore, the band at 2191 cm^{-1} characterizes CO adsorption on Ce^{4+} cations whose acidic character increased due to sulfate proximity. It is worth noting that the position of this ν(CO) band only weakly shifts under CO in the 323–623 K range (2191 cm^{-1} at 323 K to 2188 cm^{-1} at 623 K), while starting from 673 K the downwards shift is more important, and finally it reaches 2169 cm^{-1} at 773 K (Fig. 1A-Ih). This fast and strong shift is due to the reduction of both oxide and sulfate species. Regarding the sulfates, their reduction by CO starting from 673 K was evidenced from the detailed analysis of their [ν(S=O) and ν(S=O)] region. IR spectra also present a new band lying at about 2117 cm^{-1}, whose intensity increases with the temperature and which resists to an evacuation at 773 K. Binet et al. [24] assigned this band to a $Ce^{4+} \leftrightarrow Ce^{3+}$ electronic transition. The presence of this band at 423 K indicates that the ceria reduction by CO begins from 423 K but to a very limited extent. Then, the ceria reduction quickly increases above 623 K. Moreover, at T_{red} = 523 K, the band at 2356 cm^{-1} (which is due to the molecular adsorption of CO_2) provides another proof of oxygen removal from the catalyst upon CO interaction. Consistently, in regard of the intensity of this band, the amount of formed CO_2 is very important between 623 and 723 K, which perfectly corresponds to the temperature range for sulfates and oxide reduction by CO. The band at 1992 cm^{-1}, evident at 673 and 723 K and vanishing upon RT evacuation, is due to physisorbed COS. The amount of formed COS was evaluated from the integrated area of the gas phase band (2065 cm^{-1}): for the reduction of CeO_2-S by CO at 673 and 723 K, values of 4 and 6 $\mu mol\, g^{-1}$ were found respectively, which indicates that only 1% of sulfates are reduced to COS.

3.1.3. CeO_2-S thermogravimetric analysis

Fig. 2Aa reports the weight variation of CeO_2-S when heated under CO atmosphere. A slight mass gain is observed below 523 K, the sample weight then stabilizes between 523 and 653 K, while finally an important mass drop takes place in the 653–773 K range, with a maximum at 708 K as indicated by the first derivative (Fig. 3A). This large mass loss at high temperatures is not observed in the case of the non-sulfated sample (Fig. 2Be). Even if the CeO_2-S mass decreases under CO in the high temperature range, at 773 K the sample mass remains higher than after the oxidative pretreatment. Values of +13 and +2 $mg\, g^{-1}$ are measured before and after CO evacuation, respectively.

3.1.4. CeO_2-S TPR_{CO}

Fig. 4Ab shows the CO_2 evolution versus temperature when CO was flowed over CeO_2-S. Similarly to the sulfate free ceria (Fig. 4Aa), CO_2 is detected in the exhaust gas only for temperatures above 473 K. The CO_2 amount increases from 473 to 523 K and then a constant but low yield is observed until 603 K. Between 603 and 773 K, the MS signal (m/z = 44) suddenly rises to reach a maximum at 763 K. More precisely, starting from 673 K, the behavior of CeO_2-S becomes distinct from that of sulfate free ceria (Fig. 4Aa): CO_2 amount keeps on increasing in the case of CeO_2-S but decreases for CeO_2. The comparison of TPR_{CO} results for CeO_2 and CeO_2-S thus reveals that the amounts of CO_2 formed below 673 K are similar. Accordingly, we suggest that the CO_2 formation in this temperature range mainly results from oxide reduction rather than sulfate species reduction. The evaluation of the CeO_2 reduction state by IR spectroscopy (variation of the intensity of the band at ~2120 cm^{-1}) indeed provides evidence that deep ceria reduction starts at 423 K and that this phenomenon increases upon further heating (Figs. 1A-I and S1A-I). As also observed from IR, both the CeO_2 and CeO_2-S reduction by CO goes through the formation of formate and carbonate intermediates [17], which delays the CO_2 emission to higher

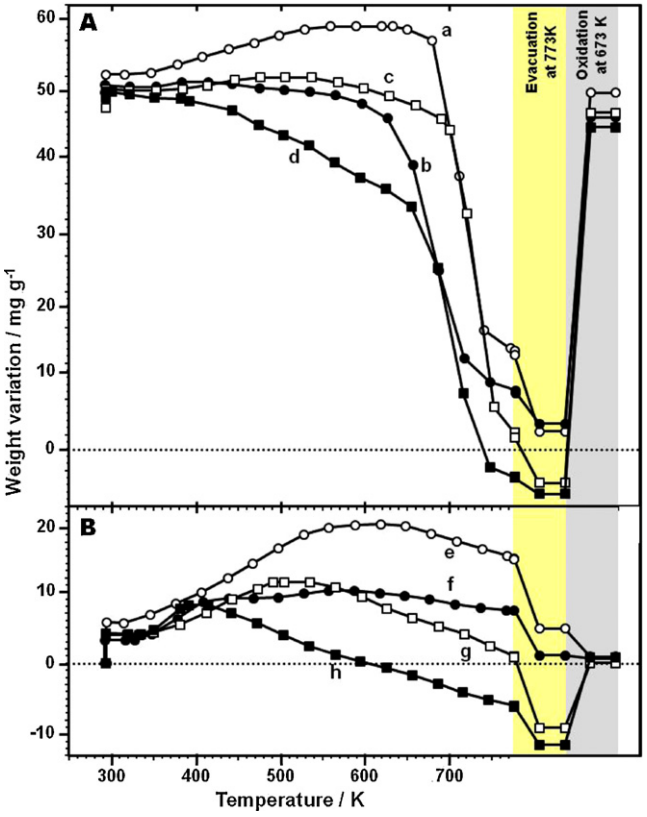

Fig. 2. Weight variation of samples upon heating under CO (2.7 kPa) from 298 to 773 K and subsequent evacuation at 773 K, followed by a re-oxidation under O_2 at 673 K. (A) Sulfated samples and (B) sulfate-free samples. (a) CeO_2-S, (b) Pt/CeO_2-S, (c) $CeZrO_2$-S, (d) Pt/$CeZrO_2$-S, (e) CeO_2, (f) Pt/CeO_2, (g) $CeZrO_2$ and (h) Pt/$CeZrO_2$.

temperatures. Furthermore, the reduction of ceria sulfate species does not seem to initiate below 673 K in regard of the surface and bulk-like sulfate band intensities (Fig. 1A-II). As a conclusion, the CO_2 emission between 673 and 773 K (Fig. 4Ab) is mainly due to sulfate reduction (important weight loss observed by thermogravimetry, full elimination of bands due to sulfate species) and to a smaller extent to the completion of the oxide reduction. Besides, the study of the CeO_2-S reducibility by CO shows that both surface and bulk-like sulfate species are reduced. The reduction process seems to proceed in two steps: at first and below 623 K only ceria

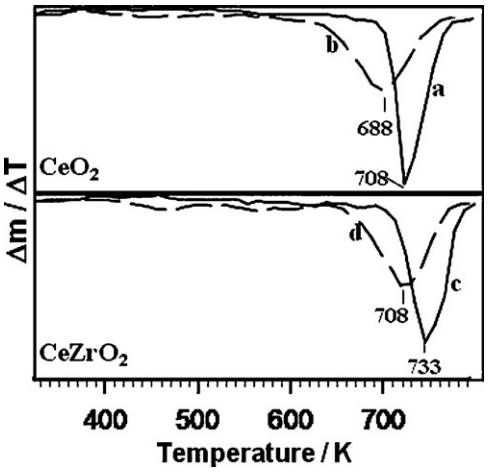

Fig. 3. First derivatives of weight variation curves depicted in Fig. 2A. (a) CeO_2-S, (b) Pt/CeO_2-S, (c) $CeZrO_2$-S and (d) Pt/$CeZrO_2$-S.

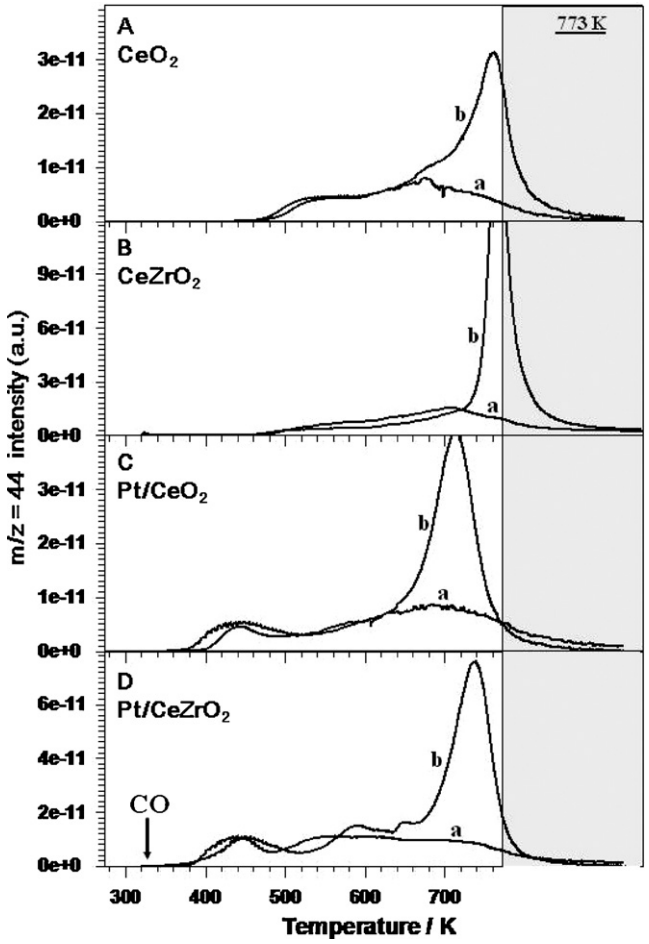

Fig. 4. TPR_{CO} curves ($m/z = 44$ signal intensity monitored by MS) of (A) CeO_2, (B) $CeZrO_2$, (C) Pt/CeO_2, (D) $Pt/CeZrO_2$ for (a) sulfate-free samples and (b) sulfated samples. The reducing flow was made of CO (5 cm^3 min^{-1}) and N_2 (25 cm^3 min^{-1}).

reduction takes place, then, above 673 K, all sulfate species are reduced while oxide reduction completes.

Using CO for CeO_2-S full reduction leads to large CO_2 emission (physisorption band at 2356 cm^{-1} and TPR_{CO}) and also to COS, but in very low proportions (band at 1992 cm^{-1} in Fig. 1A-I). The sulfur amount thus remains unbalanced and this may arise from sulfur storage onto the oxide in a non IR active form. Consecutively to the reduction step by CO, the re-oxidation of CeO_2-S was achieved at 673 K by introducing O_2 into the Mac Bain. This led to an important weight gain, as depicted in Fig. 2Aa. Consistently, IR spectroscopy illustrates the almost full recovery of sulfate bands (Fig. 5A). This experiment thus provides a clear evidence that the majority of sulfate species is reduced by CO to yield sulfur or oxysulfur species which remain on the oxide and turn back to sulfates upon O_2 re-oxidation. The sulfur amount remaining on CeO_2 together with the oxide reduction level after the CO treatment were evaluated from the thermogravimetric data according to a procedure detailed in a previous work [14]. The results will be discussed later in a dedicated part of the present paper.

3.2. Influence of platinum on sulfate reduction by CO

As described in the introduction, noble metals and principally Pt are active components of the TWCs. The following part will thus deals with the characterization of the influence of Pt on the ceria reduction process. Therefore, similar experiments to those previously described for CeO_2-S were performed over Pt/CeO_2-S.

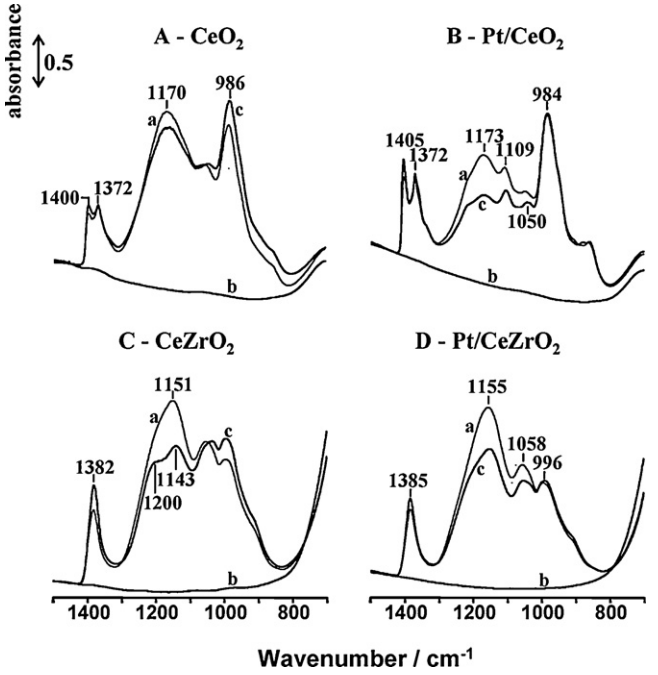

Fig. 5. IR spectra recorded after (a) sulfating at 723 K followed by (b) heating under CO and subsequent evacuation at 773 K and (c) oxidation under O_2 at 673 K. (A) CeO_2, (B) Pt/CeO_2, (C) $CeZrO_2$ and (D) $Pt/CeZrO_2$.

Fig. 1B then reports the evolution of the infrared spectra typical of Pt/CeO_2-S interacting with CO upon increasing temperature.

3.2.1. Carbonate–sulfate region (1700–800 cm^{-1} range)

The information relative to the sulfates reducibility is available from the lower wavenumber region (Fig. 1B-II). Interestingly, no significant band characteristic of formate or carbonate species is detected in contrast with what was observed with the Pt free sample (Fig. 1A-II). According to the evolution of their band intensity, both surface (1404 and 1372 cm^{-1}) and bulk-like (1170 cm^{-1}) sulfate species start to be reduced from 623 K and the remaining amount is very low at 673 K (Fig. 1B-IIe and f). Further heating under CO at 723 K leads to the complete disappearance of sulfates. IR data obtained for Pt free CeO_2-S revealed that in the absence of noble metal the sulfate reduction begins at 673 K (Fig. 1A-IIf). One can therefore conclude that platinum addition favors the sulfate reduction by CO.

3.2.2. Adsorbed CO region (2400–1900 cm^{-1} range)

Complementary information about both the metallic phase and the oxide surface properties can be obtained from the study of the 2400–1900 cm^{-1} region. The Pt/CeO_2-S treated by CO at 323 K (Fig. 1B-Ib) is characterized by bands at 2189 cm^{-1} (vanishing upon evacuation at RT) and 2149 cm^{-1} (stable upon evacuation at RT). The first peak at 2189 cm^{-1} is assigned to CO adsorbed on Ce^{4+} cationic sites. The +8 cm^{-1} shift observed, when compared with the sulfate free ceria experiment (see Supporting information, Fig. S1B-Ib) is again a consequence of an increased acidity associated to the presence of sulfate species. Concerning the presence of platinum, its interaction with CO at RT is expected to give bands in the 1930–2120 cm^{-1} spectral range. The spectrum recorded for the sulfate free ceria sample reduced by CO at 323 K (Fig. S1B-Ib) reveals three peaks located at 2111, 2070 and 1936 cm^{-1} that are assigned to linearly adsorbed CO on $Pt^{\delta+}$, Pt^0 and to bridged (Pt^0, Ce), respectively [25,26]. The presence of a peak at 2111 cm^{-1} indicates that part of platinum remains oxidized ($Pt^{\delta+}$). Oxidized platinum results from interactions of the metal particles with oxygen in the close

vicinity [23,27], indeed. The electronegative properties of oxygen render the Pt atoms slightly electron deficient, which in turn lowers the electron $2\pi^*$ back donation from Pt to CO and thus leads to an increase of the ν(CO) wavenumber. The presence of oxygen close to the metal is probably due to the migration of oxygen from the support to the platinum. Coming back to the sulfated samples, the band at 2149 cm^{-1} is not noticed for the platinum free ceria and is stable under vacuum at RT unlike those typical for CO adsorbed on a cationic site of CeO_2. Consequently, the band at 2149 cm^{-1} should correspond to CO adsorbed onto platinum and the band position would imply an oxidized state of the noble metal. The +38 cm^{-1} unusual shift observed in presence of sulfates (as mentioned above, the band is pointed at 2111 cm^{-1} for sulfate-free Pt/CeO_2, see Fig. S1B-Ib) indicates a very strong interaction between platinum and sulfate species. The sulfates may either directly form on the metal surface or on the support but nearby the platinum particles. An important enhancement of the oxidized character of Pt particles due to the presence of electronegative sulfate in the close proximity has already been noticed by infrared [28,29] but also photoelectron spectroscopy (XPS), even revealing the presence of Pt^{4+} on sulfated Pt/Al_2O_3 [30].

At T_{red} = 423 K, the CO_2 formation proceeds as revealed by the band at 2359 cm^{-1}. The electronegative effect of sulfate species again shifts this band toward higher frequencies (2349 cm^{-1} for sulfate-free samples). Regarding platinum, the corresponding bands (2141 cm^{-1} and shoulder at 2100 cm^{-1}) intensity becomes higher, thus revealing a higher Pt accessibility while keeping mainly an oxidized character. It is noteworthy to underline that for sulfate free ceria, platinum full reduction was achieved at 423 K (Fig. S1B-Ib). A further CO treatment of Pt/CeO_2-S at T_{red} = 523 K, leads to the complete reduction of platinum, as evidenced by the peak at 2082 cm^{-1} typical for CO adsorption on Pt^0. The +20 cm^{-1} shift, when compared with the peak position observed over the sulfate-free sample reduced in the same condition (Fig. S1B-Ic) is again due to the presence of sulfates. The amount of physisorbed CO_2 (2359 cm^{-1}) is high and the birth of the band at 2112 cm^{-1}, which is stable under evacuation at 523 K (spectrum d*) reflects the ceria reduction. Pursuing the heating under CO till 623 K, a high increase of the intensity of bands due to adsorbed CO_2 and to ceria reduction was noticed. In parallel, the Pt accessibility became very weak. At higher temperatures, CO treatment provoked mainly an increase of ceria reduction associated to CO_2 production and a band at 1985 cm^{-1} indicates little COS emission at 673 K.

In order to summarize, the presence of sulfate species over ceria: (i) leads to an increase of the acidity of cationic ceria sites (a shift of about +10 cm^{-1} being recorded for both CO and CO_2 adsorbed on Ce^{4+}) and (ii) delays the platinum reduction by CO, since for sulfate-free Pt/CeO_2 platinum is reduced at 423 K whereas on sulfated sample this reduction only proceeds at 523 K.

3.2.3. Pt/CeO_2-S thermogravimetric analysis

The weight variation curve for Pt/CeO_2-S heated under CO is reported in Fig. 2Ab and the corresponding first derivative in Fig. 3b. The sample mass remains almost constant below 623 K, but then an important weight loss takes place between 623 and 773 K with a variation maximum measured at 688 K (Fig. 3b). The comparison of TGA first derivatives relative to CeO_2-S (Fig. 3a) and Pt/CeO_2-S (Fig. 3b) samples clearly shows a positive effect of platinum, which favors the sulfate reduction by CO at lower temperature. Particularly, the temperature from which the reduction initiates is lowered by about 50 K and that corresponding to the maximum of the weight variation by 20 K.

3.2.4. Pt/CeO_2-S TPR_{CO}

The curves shown in Fig. 4Ca and b present the amount of CO_2 formed during the TPR_{CO} of Pt/CeO_2 and Pt/CeO_2-S, respectively. By comparison with the data reported above for platinum free CeO_2, an additional CO_2 emission peak is now observed near 423 K. The CO_2 formation thus proceeds in two steps in presence of platinum. According to the infrared results presented above, the first step which takes place between 400 and 500 K is mainly due to platinum reduction, while the more important second one (observed at higher temperatures) is due to both sulfate and ceria reduction. In the presence of sulfates or not, platinum thus leads to CO_2 emission at lower temperature. This may arise from the reaction between CO and oxygen on the platinum particle surface. This hypothesis is supported by the fact that in both sulfated and sulfate—free samples bands due to CO—O co-adsorption on platinum (described as CO-$Pt^{\delta+}$) are observed. These bands disappear upon increasing temperature (i.e. 523 K) to yield peaks typical for CO interacting with metallic Pt^0, while simultaneously the ceria reduction is revealed by the appearance of the broad electronic transition band around 2110 cm^{-1}. The ceria reduction may thus initiate in the close proximity of platinum particles and further propagate.

3.3. Influence of zirconium addition on sulfate reduction by CO

As described in Section 1, the addition of zirconium in the fluorine ceria structure leads to mixed oxides whose acid-basic and red-ox properties are both affected by changes in the oxygen mobility. The infrared spectra of $CeZrO_2$-S and $Pt/CeZrO_2$-S under CO upon increasing temperatures are reported in Fig. 1C and D, respectively.

3.3.1. Sulfated $CeZrO_2$ reduction

The main data relative to the reducibility of $CeZrO_2$-S by CO followed by infrared spectroscopy (Fig. 1C) are reported below.

3.3.1.1. Carbonate–sulfate region (1700–800 cm^{-1} range). The evolution with the temperature of the corresponding species during the $CeZrO_2$-S treatment under CO is depicted in Fig. 1C-II. The spectrum of sulfated $CeZrO_2$ shows two characteristic bands at 1383 cm^{-1} and 1151 cm^{-1} corresponding to surface and bulk-like sulfate species, respectively [13,14]. Whatever the reduction temperature, no band characteristic of carbonate or formate species is observed contrarily to what was reported in the case of the sulfate free $CeZrO_2$ (Fig. S1C-II). At a first sight, the intensity of bands assigned to sulfate species is not modified for T_{red} < 673 K. However, by comparison of spectra before and after CO reduction at 673 K (Fig. 1C-II inlet), a slight decrement of the 1383 cm^{-1} band intensity is detected. Then, upon heating up to 723 K, the whole set of bands characteristic of sulfate species disappears. This result shows that, over $CeZrO_2$, any sulfate species is reducible by CO at this temperature (723 K). In similar conditions, the sulfate species formed over CeO_2 (Fig. 1A-II) seem to be more easily removed because at 673 K the intensity of sulfate species bands had already strongly decreased.

3.3.1.2. Adsorbed CO region (2400–1900 cm^{-1} range). Regarding the CO interaction with the mixed oxide cationic sites, a positive shift (+10 cm^{-1}) is again observed when compared with the sulfate free $CeZrO_2$ sample, as expected from the support acidity increase upon sulfates deposition (Figs. 1C-Ib and S1C-Ia). The initial band position (2191 cm^{-1} from 323 to 623 K) typical for this CO interaction with cationic sites again shifts toward lower wavenumber upon increasing temperature (2174 cm^{-1} after CO treatment at 773 K). This indicates that the cerium cation reduction proceeds, as also evidenced by the band at 2117 cm^{-1} whose appearance at 623 K confirms that the oxide reduction initiates at this temperature. Both the oxide and the sulfate reduction then proceed at higher

temperatures, as evidenced by the COS peak (1997 cm^{-1}) at 723 K and the huge amount of adsorbed CO_2 (2359 cm^{-1}).

3.3.1.3. $CeZrO_2$-S thermogravimetric analysis. The mass variation curve corresponding to $CeZrO_2$-S heated under CO from 293 to 773 K is reported in Fig. 2Ac. Just like CeO_2-S, the main mass loss is observed in the 700–750 K range. Nevertheless, the comparison of the first derivative curves (Fig. 3c) clearly shows an effect of Zr addition to ceria. Indeed, the maximum weight variation is pointed at 708 K for CeO_2-S but 733 K for $CeZrO_2$-S. Both thermogravimetric and spectroscopic results thus indicate that the sulfate reducibility by CO operates at lower temperature over CeO_2 than over $CeZrO_2$ (the temperature gain is about 25 K). Therefore, the weak amplitude mass loss observed by thermogravimetry in the 550–680 K temperature range may be considered as a fingerprint of the oxide reduction only. On the contrary, the important weight loss observed between 683 and 773 K is mainly due to the sulfates reduction, with however a concomitant oxide reduction.

3.3.1.4. $CeZrO_2$-S TPR_{CO}. Fig. 4B confirms the previous conclusion. The slight CO_2 evolution in the low temperature range is indeed similar to that observed with the sulfate free mixed oxide, while the main CO_2 evolution for $CeZrO_2$-S is detected above 700 K when sulfates are removed.

3.3.2. Sulfated $Pt/CeZrO_2$ reduction

The reducibility of $Pt/CeZrO_2$-S by CO was followed by infrared spectroscopy (Fig. 1D) and the main data are reported below.

3.3.2.1. Carbonate–sulfate region (1700–800 cm^{-1} range). The two bands at 1385 and 1155 cm^{-1} (Fig. 1D-IIa) characterize surface and bulk-like sulfate species, respectively. No modification of these sulfates bands (intensity and position) was observed after a treatment under CO at 323 K and 423 K. A weak decrease of both intensity and wavenumber of the ν(S=O) frequency at 1385 cm^{-1} is noted after treatments at 523, 623 and 673 K (see Fig. 1D-II inlet). At 673 K, the intensity of the band at 1155 cm^{-1} due to ionic sulfate species also significantly decreased. Finally, no significant band due to sulfate species is observed after a treatment at 723 K, showing the ability of CO to reduce the totality of sulfate species formed over $Pt/CeZrO_2$ at this temperature.

3.3.2.2. Adsorbed CO region (2400–1900 cm^{-1} range). A shift of +9 cm^{-1} is observed for the band assigned to CO adsorbed on cationic sites (2191 cm^{-1}) when compared with the sulfate free $Pt/CeZrO_2$ (Figs. 1D-Ia and S1D-Ia). A similar effect was previously reported for the ceria experiments and related to an increased acidity when sulfates are formed. A downward shift of this band is observed upon heating the sample under CO (2175 cm^{-1} at 773 K, Fig. 1D-Ih). This phenomenon is due to the decrease of the cation Lewis acidity provoked by the reduction of both oxide and sulfate species. Regarding the CO interaction with platinum, only one band is detected at T_{red} = 323 K (Fig. 1D-Ia). The corresponding high wavenumber (2150 cm^{-1}) characterizes a $Pt^{\delta+}$ platinum species strongly perturbed by the electron acceptor effect of neighboring sulfate species. At 423 K the intensity of this band significantly increases and the appearance of a new peak at 2080 cm^{-1} is observed. This later band reveals the formation of reduced platinum (Pt^0) for which the preliminary sulfating effect is very weak, since for the same CO treatment temperature the sulfate free $Pt/CeZrO_2$ had led to an almost identical band at 2078 cm^{-1} (Fig. S1D-I). Hypothesizing an increasing inductive sulfate effect in the proximity of the metal, the CO treatment at 423 K would thus not only initiate the platinum reduction but also that of the sulfates species at the close vicinity of the metallic particles. This hypothesis is consistent with the slight intensity loss of the 1385 cm^{-1} band (typical for surface sulfates) which was reported above in the same temperature range. When the reduction temperature reaches 523 K, the platinum only remains in the Pt^0 form (only one residual band at 2080 cm^{-1}). According to the intensity evolution of this band, the amount of CO interacting with platinum decreases strongly at 623 K and, at higher temperatures, no interaction is clearly evidenced. The evolution of the oxide reduction was furthermore followed thanks to the evolution of the ~2111 cm^{-1} band intensity. The oxide reduction seems to initiate at 523 K and further proceed until 773 K. It is however quite difficult to assess whether or not the reduction begins at lower temperature (323–423 K) by this mean, since an overlapping band at 2150 cm^{-1} (due to CO adsorbed on $Pt^{\delta+}$) is present. The two bands at 2360 and 1997 cm^{-1}, already observed previously, and which easily vanish upon evacuation at room temperature, are due to physisorbed CO_2 and COS, respectively. Carbon dioxide is, therefore, mainly formed between 523 and 723 K, while COS is only observed at 673 and 723 K.

3.3.2.3. $Pt/CeZrO_2$-S thermogravimetric analysis. The $Pt/CeZrO_2$-S mass variation curve upon heating under CO is composed of three main domains (Fig. 2Ad). Firstly, in the lower temperature range (T < 410 K), no significant changes are observed. Then, a continuous weight decrease (6×10^{-2} mg/K) is detected in the 410–640 K range. The observed mass loss in this domain is due to: (i) the reduction of the platinum particles, as previously evidenced from CO adsorption first on $Pt^{\delta+}$ (band at 2150 cm^{-1}), then on Pt^0 (2080 cm^{-1}); (ii) the initiation of the mixed oxide reduction, as evidenced by the emerging band at 2111 cm^{-1}; (iii) the reduction of a small proportion of surface sulfate species [lowering of the 1385 cm^{-1} ν(S=O) band intensity]. Finally, a rapid mass loss follows until 740 K. This later is due to the full reduction of both the mixed oxide and the totality of the surface and bulk-like sulfate species. The maximum of weight variation determined via the first derivative curve (Fig. 3d) is detected at 708 K. The comparison of the derivative curves clearly shows an effect of Zr addition to ceria. Indeed, the maximum of weight variation is pointed at 688 K for Pt/CeO_2-S and at 708 K for $Pt/CeZrO_2$-S. The Zr addition effect is thus similar for samples with or without platinum: the maximum of weight variation is about 20–25 K upward shifted. An identical phenomenon was observed during the H_2 reduction of sulfated $Ce_XZr_{1-X}O_2$ solids [14]. It was proposed that the addition of zirconium renders the interaction with bulk-like sulfate species stronger and thus makes their migration toward the surface more difficult.

3.3.2.4. $Pt/CeZrO_2$-S TPR_{CO}. In comparison with the sulfate-free $Pt/CeZrO_2$ (Fig. 4 Da), the TPR_{CO} measurement (Fig. 4Db) indicates that the reduction of sulfated mixed oxide $Pt/CeZrO_2$-S by CO also leads to CO_2 formation between 410 and 773 K but with an additional intense CO_2 release starting from 673 K, which corresponds to the sulfate reduction as described above.

3.4. Sulfur storage upon sulfate reduction by CO

Consecutively to the reduction by CO and further evacuation of sulfated samples at 773 K, the introduction of dioxygen in the thermobalance at 673 K led to a mass gain for any of the Ce-based samples (Fig. 2A). Whatever the oxide composition, similar experiments performed in the infrared cell led to both the reappearance of the sulfate species bands (Fig. 5) and the complete disappearance of the 2111 cm^{-1} band (range not shown). These observations indicate that all the oxides are completely re-oxidized by an oxygen treatment at 673 K and that sulfur was stored on/in the oxide. Sulfur is indeed mainly stored in the form of CeO_2-S and Luo and Gorte reported that CeO_2-S can easily be re-oxidized by O_2 [31]. The amount of stored sulfur was evaluated using a gravimetric method described in a previous paper dealing with sulfates reduction under

Table 2
Quantitative values of sulfur storage on the samples and oxygen removal from thermogravimetric measurements.

Samples	Sulfation[a]		CO reduction[b]	
	Sulfate storage (μmol g^{-1})	Sulfur storage (μmol g^{-1})	Oxide reduction	
			O_{atomic} removal (μmol g^{-1})	x in Ce(Zr)O_x
CeO_2	–	–	[c]	[c]
CeO_2-S	617	606	1059	1.82
Pt/CeO_2	–	–	[c]	[c]
Pt/CeO_2-S	616	557	893	1.85
$CeZrO_2$	–	–	568	1.91
$CeZrO_2$-S	595	576	1446	1.78
Pt/$CeZrO_2$	–	–	663	1.90
Pt/$CeZrO_2$-S	604	545	1483	1.77

[a] Sulfating under SO_2 (600 μmol g^{-1}) and O_2 (6.5 kPa): values determined at the steady state (when no mass variation was recorded) at 723 K.
[b] Reduction under CO (2.7 kPa): values determined at the steady state (when no mass variation was recorded) at 773 K.
[c] Not available as some carbonate species were still detected after the cleaning treatment.

H_2 [14]. The results reported in Table 2 show that after the CO treatment around 606, 557, 576 and 545 μmol g^{-1} of sulfur were stored on CeO_2-S, Pt/CeO_2-S, $CeZrO_2$-S and Pt/$CeZrO_2$-S respectively. These values reveal that, for Pt-free compounds, about 98% of sulfate species are reduced to stored sulfur under CO, while the extent of sulfate reduction to sulfur is limited to 90% for platinum loaded oxides. By comparison, the sulfur storage level determined similarly for sulfated samples reduced under hydrogen was significantly less important [14]. In that case, about 75% of ceria sulfates was reduced to form sulfur and only 60% for $CeZrO_2$ samples. It was found in that case that the amount of stored sulfur after an H_2 treatment is closely related to the sample specific surface area and that the presence of platinum does not affect noticeably the sulfur-storage. In the present case for which the reducing treatment was made under CO, the amount of sulfur stored upon sulfate species reduction is markedly more important and clearly not correlated to the surface area of the sample.

3.5. OSC of sulfated Ce-containing samples

The OSC (redox capacity) of sulfated Ce-based catalysts at 773 K was assessed using the thermogravimetric data. The thermogravimetric analysis was indeed described as a reliable method for the evaluation of sulfated ceria–zirconia mixed oxides OSC. Table 2 summarizes the OSC values determined using the method reported in Ref. [14]. The OSC evaluations at 773 K are 1059, 893, 1446 and 1483 μmol g^{-1} of atomic oxygen for CeO_2-S, Pt/CeO_2-S, $CeZrO_2$-S and Pt/$CeZrO_2$-S respectively. Table 2 also reports the OSC for sulfate-free $CeZrO_2$ samples; the obtained values are 568 and 663 μmol g^{-1} of atomic oxygen for $CeZrO_2$ and Pt/$CeZrO_2$ respectively. The OSC values for pure ceria compounds were impossible to estimate due to presence of carbonate species remaining even after the cleaning treatment.

The OSC values reported here for the sulfated samples are much higher than those for the sulfate-free samples. A similar observation was reported by Luo and Gorte [32] using pulse–reactor techniques. They concluded that sulfur poisoning gives rise to an apparent increase in oxygen storage for CeO_2 based material. This higher OSC could also possibly be due to the replacement of some atomic oxygen by atomic sulfur in the oxide lattice (i.e. formation of an oxysulfide), resulting in a higher effective oxygen capture/release in the case of the sulfur/sulfated materials. Alternatively, this higher OSC could also result from the (reversible) oxygen removal from sulfates, giving rise to elemental sulfur residue on the sample, as evidenced by the re-oxygenation experiments (Section 3.1). However, the OSC evaluated here for CO reduced samples are sensitively higher than those reported for H_2 reduction [14]. The OSC increase is roughly 200 μmol g^{-1} and this value is closed to the additional amount of stored sulfur. This is a further element indicating that the oxygen capture/release is promoted by the sulfur/sulfates stored on the oxides. The OSC of sulfated samples with and without Pt are very close, therefore a particular influence of the metallic phase was not observed.

3.6. Proposed mechanism for sulfate reduction

The whole experimental results reported above clearly show that platinum addition on Ce-based compounds favors the reduction of sulfate species by CO. It is well known that the presence of Pt favors the sulfate reduction by H_2. In that case, it was proposed that the dissociation of molecular hydrogen onto the metal leads to the formation of atomic hydrogen which is more reactive toward adsorbed surface species [14]. The proposed mechanism for sulfate reduction by hydrogen thus includes the following five main steps. (I) The H_2 dissociation first takes place over Pt and is followed by atomic hydrogen spill-over on the surface. (II) The oxide reduction then operates. (III) The surface sulfate reduction by atomic hydrogen then proceeds at lower temperature than when using H_2 over Pt free oxides. Moreover, the sulfates are more easily reduced over previously reduced oxides. (IV) The elimination of sulfate species from the surface leads to a surface–bulk unbalance which is then corrected by sulfate migration from the bulk to the surface. This migration might occur only above a threshold temperature evaluated around 673 K. (V) The direct sulfate reduction by H_2 finally takes place.

In the context of the present work, the positive platinum effect on the sulfates reduction by CO cannot be explained by a CO spill-over on the oxide surface contrarily to what was proposed with H_2. However, the results presented above indicate that the sulfates reduction mechanism using CO also involves a migration step between bulk-like and surface sulfate species (Fig. 6, step III). Moreover, the sulfates reduction occurs simultaneously with the reduction of the Ce-containing oxides: surface sulfate species would be more easily reduced by CO on pre-reduced oxide, as it was observed with H_2 (Fig. 6, step II). Recently, Happel et al. have found by radiation photoelectron spectroscopy that a reduced CeO_{2-X} surface was more active toward cleavage of S—O bonds [33]. Therefore, one may propose that platinum would favor the oxide reduction at the metal-oxide interface to yield CO_2 arising from CO adsorbed on the metal and a neighboring superficial oxygen from the Ce-containing oxide (Fig. 6, step I). As a consequence, sulfates will start to decompose to provide oxygen to the reduced oxide. Fig. 6 depicts the theoretical weight variation curves for oxides with (B) and without platinum (A) versus the temperature. Thus, two steps for the sulfates reduction by CO are observed over platinum loaded oxides (Fig. 6, curve B). The first step (mass loss), observed at lower temperature is characterized by the reduction of both the platinum phase and a small proportion of the surface sulfate species. The

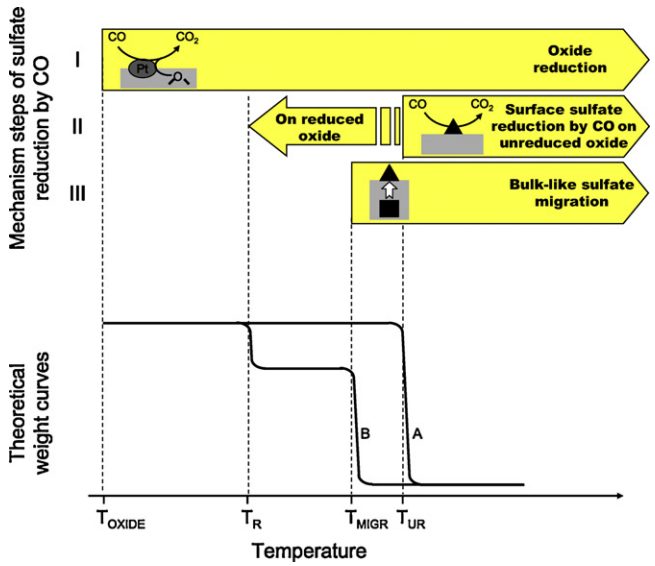

Fig. 6. Schematic representation of a proposed mechanism for sulfates reduction by CO. Top part: main steps of the mechanism. Black triangle: surface sulfates; black square: bulk-like sulfates. Bottom part: theoretical weight variation of sulfated samples upon increasing temperature under CO. (A) Pt free, Ce-containing sample; (B) Pt loaded, Ce-containing sample. T_{OXIDE} stands for oxide reduction temperature, T_R for surface sulfate reduction temperature on reduced samples, T_{MIGR} for bulk-like sulfate migration temperature and finally, T_{UR} for surface sulfate reduction temperature on unreduced samples.

second step is due to the full reduction of the oxide and both surface and bulk-like sulfate species. This second step is mainly controlled by the sulfate migration from the bulk to the oxide surface. Contrarily, only one step is observed for Pt free catalysts (Fig. 6, curve A). In this case, we propose that the reduction is connected with the own reducibility of the surface sulfate species upon direct interaction with CO. It is very interesting to underline that the reduction of sulfate species formed on Pt-free samples occurs in the 700–750 K range both for CO and H_2. Indeed, the weight variation maxima for CeO_2-S and $CeZrO_2$-S are pointed at 733 K and 753 K when reduced by H_2 [14], and at 708 K and 733 K when reduced by CO (Fig. 3). In such a case the reducing agent activation by the metal is absent, therefore the reduction is only dependent on the intrinsic properties of the material, i.e. on its capacity to retain coordinated species (depending on the acid–base and redox properties, essentially) and to oxidize the reducing agent. The weight variation maximum is thus shifted toward higher temperature (about 20–25 K) by Zr addition whatever the reducing agent, but also by the replacement of CO by H_2 whatever the oxide support. The surface sulfates supported on ceria are thus more reactive than those on $CeZrO_2$ and CO appears as a better sulfate reducing agent than H_2.

4. Conclusion

This study dealing with the sulfate reduction by CO over ceria–zirconia mixed oxides leads to the following conclusions:

1. The proposed mechanism for sulfate reduction by CO involves a migration step between bulk-like and surface sulfate species. The sulfate reduction occurs at the oxide surface and consecutively the bulk-like species migrate toward the surface vacant sites. The bulk can thus be considered as a sulfate reservoir.
2. The reduction of sulfated Pt-free samples occurs in only one step and is connected with the own reducibility of the surface sulfate species upon direct interaction with CO. A detailed analysis indicates that the surface sulfates supported on CeO_2 are more reactive than those on $CeZrO_2$ and that CO is a better reducing agent than H_2.
3. The platinum addition favors the reduction of sulfate species by CO over all the Ce-based compounds and the surface sulfate species appear to be more easily reduced by CO over the reduced oxides. Therefore, the platinum promoting effect would be directly related to the better oxide reducibility in presence of the metallic phase. Two steps for sulfate reduction by CO are indeed observed for platinum loaded oxides. The first step at lower temperature is characterized by the reduction of both the platinum phase and a small proportion of the surface sulfate species. The second step, which corresponds to the full reduction of the oxide and both surface and bulk-like sulfate species, appears to be mainly controlled by the migration of sulfate species from the bulk to the oxide surface.
4. Consequently to the sulfates reduction, sulfur is stored on platinum [12] but also onto the oxide probably in the form of a cerium oxysulfide or as an elemental sulfur layer at the surface. The amount of stored sulfur was evaluated by a gravimetric method enabling to assess that over Pt-free oxides about 98% of sulfate species are converted, under CO atmosphere, to stored sulfur. When Pt is present the sulfate removal through the elimination of gaseous compounds (COS) increases and 'only' 90% of the original amount remain in the sulfur form. Moreover, the amount of sulfur stored after sulfate species reduction with CO is markedly more important than that after reduction with H_2 and is clearly not correlated with the sample surface area.
5. The CO reduction of sulfated Ce-containing oxides leads to the formation of only a small amount of gaseous COS, which is consistent with a high amount of stored sulfur.
6. The oxide reduction is always concomitant to the sulfates one and is therefore linked to the oxygen mobility. The sulfated Ce-based catalyst OSC was assessed at 773 K using thermogravimetric measurements. The OSC for mixed oxides is greatly enhanced after sulfate deposition and furthermore the OSC measured after CO reduction is sensitively higher than that reported after H_2 reduction. This higher OSC could be due to the replacement of some atomic oxygen by atomic sulfur in the sample lattice (i.e. formation of an oxysulfide), or more simply to the removal of oxygen atoms from the SO_x moieties (leading to sulfur species deposit), resulting in a higher effective oxygen release/capture in the case of the sulfated/sulfur materials. The platinum addition does not change significantly the OSC for sulfated Ce-based oxides.

Appendix A. Supplementary data

Supplementary data associated with this article can be found, in the online version, at doi:10.1016/j.apcatb.2012.02.037.

References

[1] H.S. Gandhi, A.G. Piken, M. Shelef, R.G. Delesh, SAE Tech. Paper 760201, 1976.
[2] A. Trovarelli, Catal. Rev. – Eng. 38 (1996) 439.
[3] M. Pijolat, M. Prin, M. Soustelle, O. Touret, P. Nortier, J. Chem. Soc., Faraday Trans. 91 (1995) 3941.
[4] M. Ozawa, J. Alloys Compd. 272 (1998) 886.
[5] J.R. González-Velasco, M.A. Gutiérrez-Ortiz, J.-L. Marc, Juan A. Botas, M.P. r González-Marcos, G. Blanchard, Appl. Catal. B: Environ. 22 (1999) 167.
[6] P. Fornasiero, G. Balducci, R. Di Monte, J. Kašpar, V. Sergo, G. Gubitosa, A. Ferrero, M. Graziani, J. Catal. 164 (1996) 173.
[7] P. Fornasiero, J. Kaspar, V. Sergo, M. Graziani, J. Catal. 182 (1999) 56.
[8] Y.J. Mergler, A. van Aalst, J. van Delft, B.E. Nieuwenhuys, Appl. Catal. B: Environ. 10 (1996) 245.
[9] R. Burch, J.P. Breen, F.C. Meunier, Appl. Catal. B: Environ. 39 (2002) 283.
[10] L. Kylhammar, P.-A. Carlsson, H.H. Ingelsten, H. Grönbeck, M. Skoglundh, Appl. Catal. B: Environ. 84 (2008) 268.
[11] M. Waqif, P. Bazin, O. Saur, J.C. Lavalley, G. Blanchard, O. Touret, Appl. Catal. B: Environ. 13 (1997) 265.

[12] P. Bazin, O. Saur, J.C. Lavalley, G. Blanchard, V. Visciglio, O. Touret, Appl. Catal. B: Environ. 11 (1997) 193.
[13] P. Bazin, O. Saur, J.C. Lavalley, A.M. Le Govic, G. Blanchard, Stud. Surf. Sci. Catal. 116 (1998) 571.
[14] P. Bazin, O. Saur, F.C. Meunier, M. Daturi, J.-C. Lavalley, A.-M. Le Govic, V. Harlé, G. Blanchard, Appl. Catal. B: Environ. 90 (2009) 368.
[15] M.P. Yeste, J.C. Hernandez, S. Bernal, G. Blanco, J.J. Calvino, J.A. Perez-Omil, J.M. Pintado, Catal. Today 141 (2009) 409.
[16] T. Luo, J.M. Vohs, R.J. Gorte, J. Catal. 210 (2002) 397.
[17] A. Badri, J. Lamotte, J.C. Lavalley, A. Laachir, V. Perrichon, O. Touret, G.N. Sauvion, E. Quémére, Eur. J. Solid State Inorg. Chem. 28 (1991) 445.
[18] C. Li, Y. Sakata, T. Arai, K. Domen, K. Maruya, T. Onishi, J. Chem. Soc., Faraday Trans. 85 (1989) 929.
[19] J.F. Joly, N. Zanier-Szydlowski, S. Colin, F. Raatz, J. Saussey, J.C. Lavalley, Catal. Today 9 (1991) 31.
[20] C. Binet, A. Jadi, J.C. Lavalley, J. Chim. Phys. Phys. Chim. Biol. 89 (1992) 1779.
[21] A. Badri, C. Binet, J. Saussey, J.C. Lavalley, Mikrochim. Acta 14 (Suppl.) (1997) 697.
[22] A. Badri, Thèse, Caen, 1994.
[23] D. Spielbauer, G. Mekhemer, M. Zaki, H. Knözinger, Catal. Lett. 40 (1996) 71.
[24] C. Binet, A. Badri, J.C. Lavalley, J. Phys. Chem. 98 (1994) 6392.
[25] V. Perrichon, L. Retailleau, P. Bazin, M. Daturi, J.C. Lavalley, Appl. Catal. A: Gen. 260 (2004) 1.
[26] P. Bazin, O. Saur, J.C. Lavalley, M. Daturi, G. Blanchard, Phys. Chem. Chem. Phys. 7 (2005) 187.
[27] D.W. Daniel, J. Phys. Chem. 92 (1988) 3891.
[28] J.M. Grau, J.C. Yori, C.R. Vera, F.C. Lovey, A.M. Condó, J.M. Parera, Appl. Catal. A 265 (2004) 141.
[29] L. Zhang, D. Weng, B. Wang, X. Wu, Catal. Commun. 11 (2010) 1229.
[30] G. Corro, J.L.G. Fierro, V.C. Odilon, Catal. Commun. 4 (2003) 371.
[31] T. Luo, R.J. Gorte, Catal. Lett. 85 (2003) 139.
[32] T. Luo, R.J. Gorte, Appl. Catal. B: Environ. 53 (2004) 77.
[33] M. Happel, Y. Lykhach, N. Tsud, T. Skala, K.C. Prince, V. Matolín, J. Libuda, J. Phys. Chem. C 115 (2011) 19872.